Journal of Instrumentation

Very high energy calibration of silicon Timepix detectors

Published by IOP Publishing for Sissa Medialab

Received: *August 23, 2018*
Accepted: *November 8, 2018*
Published: *November 19, 2018*

Very high energy calibration of silicon Timepix detectors

S.P. George,[1,a,b,c] **M. Kroupa,**[a,d] **S. Wheeler,**[a] **S. Kodaira,**[e] **H. Kitamura,**[e] **L. Tlustos,**[f] **T. Campbell-Ricketts,**[a,c] **N.N. Stoffle,**[a,d] **E. Semones**[a] **and L. Pinsky**[c]

[a] *Space Radiation Analysis Group, NASA Lyndon B. Johnson Space Center, 2101 E NASA Pkwy, Houston, Texas 77058, U.S.A.*
[b] *Department of Health and Human Performance, University of Houston, 4800 Calhoun Rd, Houston, Texas 77004, U.S.A.*
[c] *Department of Physics, University of Houston, 4800 Calhoun Rd, Houston, Texas 77004, U.S.A.*
[d] *Leidos Corporation, 2625 Bay Area Blvd, Houston, Texas 77058, U.S.A.*
[e] *National Institute of Radiological Sciences, Inage Ward, 4 Chome-9-1 Anagawa, Chiba, Japan*
[f] *Microelectronics Section, CERN, Route de Meyrin 385, Geneva, Switzerland*

E-mail: stuart.george@nasa.gov

Abstract: We investigate energy measurements in Timepix hybrid detectors in hole collection mode above pixel input energy depositions of about 2.2 MeV or 600,000 electron/hole pairs in Silicon. Measurement of the detector response well above this regime is important for our application measuring the heavy ion exposure of NASA astronauts. We find that high input charges produce a double pulse structure in the Timepix front end which creates a taxonomy of different clusters which are observed at accelerators, but not in typical operation on orbit. We investigate the LET response of the Timepix to different heavy ion species and find that for a given polar angle the so called 'volcano effect' can be compensated with a simple power law model. We also characterize the pixel response of the Timepix using mono-energetic stopping protons and derive a per pixel calibration method for correction of the pixel response up to about 8 MeV. We conclude that with an appropriate calibration procedure the Timepix can correctly measure the LET values in excess of 500 keV μm^{-1} in Silicon for tracks with a polar angle exceeding 60°, corresponding to the entirety of the cosmic ray spectrum up to Nickel.

Keywords: Instrumentation for heavy-ion accelerators; Pattern recognition, cluster finding, calibration and fitting methods; Particle tracking detectors; Dosimetry concepts and apparatus

[1] Corresponding author.

https://doi.org/10.1088/1748-0221/13/11/P11014

2018 JINST 13 P11014

Contents

2018 JINST 13 P11014

1 Introduction

This paper details investigations undertaken into the so called 'volcano effect' present in silicon Timepix hybrid pixel detectors operating in hole collection mode. This saturation like effect causes substantially lowered measurement of input charges in a pixel above 2.2 MeV. Compensating for this effect improves the response of the Timepix detector. This is particularly beneficial for our application which is the measurement of mixed ion fields on spacecraft for astronaut radiation monitoring.

1.1 Use of hybrid pixel detectors in space

Hybrid pixel detectors such as the Timepix [1–3] detector produced by the CERN based Medipix2 collaboration have many significant advantages for use in the characterization of mixed radiation fields such as the one in space. These include low weight, compactness, and low power consumption, all of which are typically about an order of magnitude better than other comparable systems current used in space. Other key characteristics are the ability to measure a track for the incoming particle which can be analyzed to reveal geometric information, the ability to measure incoming radiation over a full 4π solid angle and good performance at high count rates. For these reasons Timepix hybrid pixel detectors are now being used by NASA in several space applications. These include the current deployment of multiple Timepix detectors as radiation monitors on the International Space Station [4], the BIRD instrument as a payload on Orion ETF-1 [5], the HERA instrument which forms part of the Orion radiation system and is expected to fly on Orion Exploration Mission 1 onwards [6] and the planned flights of 3 Timepix detectors as part of the Bio-Sentinel project [7].

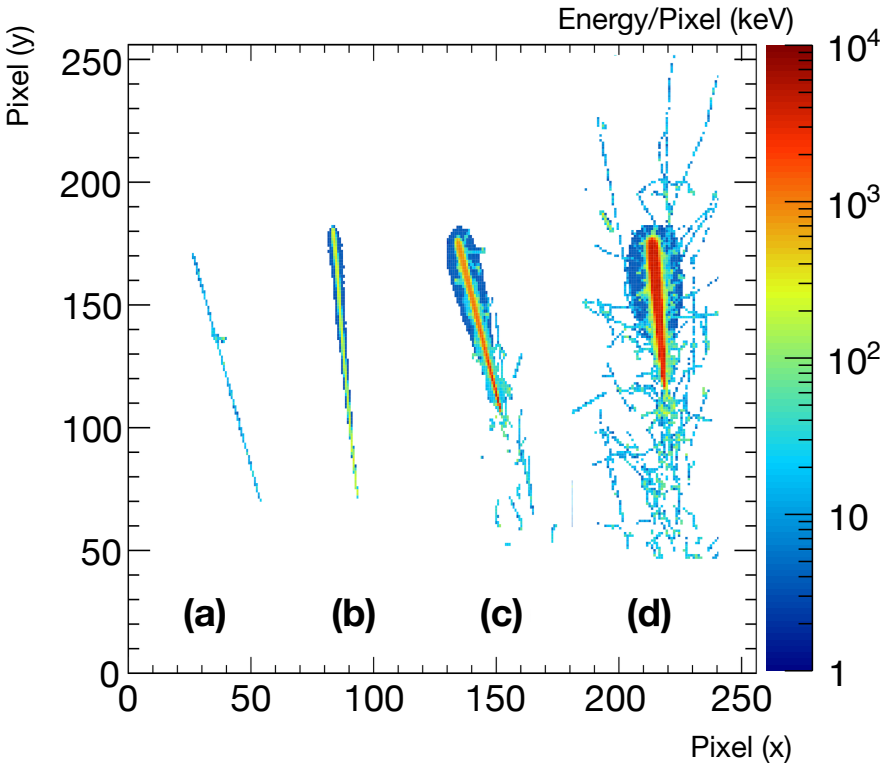

Figure 1. Four tracks of increasing LET with similar azimuth angle θ and polar angle ϕ:

(a)	$\mathrm{LET_{Si}} = 0.52\,\mathrm{keV\,\mu m^{-1}}$	$\theta = 71.0°$	$\phi = 84.6°$
(b)	$\mathrm{LET_{Si}} = 5.45\,\mathrm{keV\,\mu m^{-1}}$	$\theta = 82.0°$	$\phi = 84.0°$
(c)	$\mathrm{LET_{Si}} = 54.8\,\mathrm{keV\,\mu m^{-1}}$	$\theta = 66.7°$	$\phi = 81.4°$
(d)	$\mathrm{LET_{Si}} = 233\,\mathrm{keV\,\mu m^{-1}}$	$\theta = 84.2°$	$\phi = 81.1°$

1.2 The Timepix detector

The Timepix detector consists of a pixellated silicon sensor of 256 × 256 pixels attached to an underlying Timepix Application Specific Integrated Circuit (the Timepix ASIC). The pixels have a pitch of 55 µm and the sensor can be of variable thickness, typically 300 µm or 500 µm. Each sensor pixel is individually bump bonded to a corresponding pixel in the Timepix ASIC. The Timepix ASIC contains pulse processing electronics for each pixel consisting of a preamplifier, shaping circuit, threshold discriminator and digital counter. When operated as a Wilkinson type ADC in the 'Time-Over-Threshold' mode this enables the chip to measure deposited energy in each pixel.

When a charged particle traverses the sensor it produces a cluster of pixel hits. In this way hybrid pixel detectors such as the Timepix act like solid state nuclear emulsion. This cluster corresponds to the particle's track in silicon convolved with the subsequent charge transport through the silicon sensor and signal induction on the pixel electrode. This cluster can then be analyzed to calculate its parameters such as its length in silicon, energy deposition and track polar angles [8–10]. In turn these parameters can be used to calculate quantities directly relevant to astronaut health such as Linear Energy Transfer (LET) and an estimate of particle charge and velocity. Examples of 4 different tracks with different measured stopping powers and similar polar angles are shown in figure 1.

2018 JINST 13 P11014

One important quantity measured by these detectors many applications is the LET in silicon which is calculated as the quotient of the total track energy and the total track length in the silicon detector. This quantity is similar but not identical to the stopping power $\frac{dE}{dX}$, especially for high energy and charge ions, where delta electrons and bremsstrahlung photons may leave the sensor. Timepix is capable of correctly measuring LET for the vast majority of charged particles in space, having an approximate maximum LET measurement value of 80 keV µm^{-1}. This range covers the majority of the cosmic ray spectrum up to $Z \approx 14$, comprising some 99.9% of cosmic rays [11]. However its suffers from a saturation effect called the Volcano Effect when energies higher than about 2.2 MeV are deposited in a single pixel. Energy depositions exceeding this value can be found for slow ions heavier than carbon and are routine for ions heavier than magnesium. Despite the relatively low number of these ions in the cosmic ray field recent research has indicated that heavy ions may have outsized biological effect [12], and so accurately measuring the stopping power up to very high LET values such as 500 keV µm^{-1} which are typical of ions such as ^{56}Fe and ^{60}Ni is important for precise space radiation dosimetry.

In a silicon sensor this a 2.2 MeV energy deposit creates 600,000 electron/hole pairs at 3.62 eV per electron hole pair. These electron hole pairs are then swept out by the applied bias voltage and a signal is subsequently induced by these traveling charges in the electrodes of the pixel matrix. While in principal recombination effects may also affect LET measurement, previous investigations in the literature [13, 14] only report the presence of these effects at LET values much greater than those encountered in this study. As such one would expect the volcano effect to be a phenomenon of the Timepix ASIC, not some more fundamental effect involving the physics of silicon detectors. As all of our experimental effort is carried out with hole collecting silicon sensors, for the rest of this article we refer to the energy deposit in eV rather than the number of electron/hole pairs created in the sensor.

We note that the results shown in this paper should be generally applicable to any hole collecting sensor attached to a Timepix ASIC and that an additional benefit of this work is that extending the high energy response of the Timepix may also be useful for other applications which input large quantities of charge into a pixel over very short time scales. Some examples of these applications are measurements with free electron lasers and pulsed neutron sources.

1.3 The volcano effect

The volcano effect is named after its visible manifestation, which is a caldera like hollowing out of the measured energy deposition in the center of a cluster and a net loss of total measured energy deposition with respect to what would be theoretically expected. It has been discussed in a number of articles [8, 15] and has only been observed for Timepix detectors operating in hole collection mode, with Timepix detectors collecting electrons seeming to instead exhibit clusters with a ‘flat top’ [16]. An example of a typical volcano effect cluster is shown in figure 2.

In this article we investigate and characterize the volcano effect in several ways. Firstly we characterize the response of the pixel front end using by connecting an oscilloscope to the preamplifier and comparator outputs. This shows that the volcano effect is in fact a saturation effect in the pixel ASIC resulting from an unusual ‘double pulse’ response of the preamplifier. This double pulse structure leads to a family of different clusters for the same primary ion which can be observed at accelerators, but most of which are not relevant to our application in space. We

2018 JINST 13 P11014

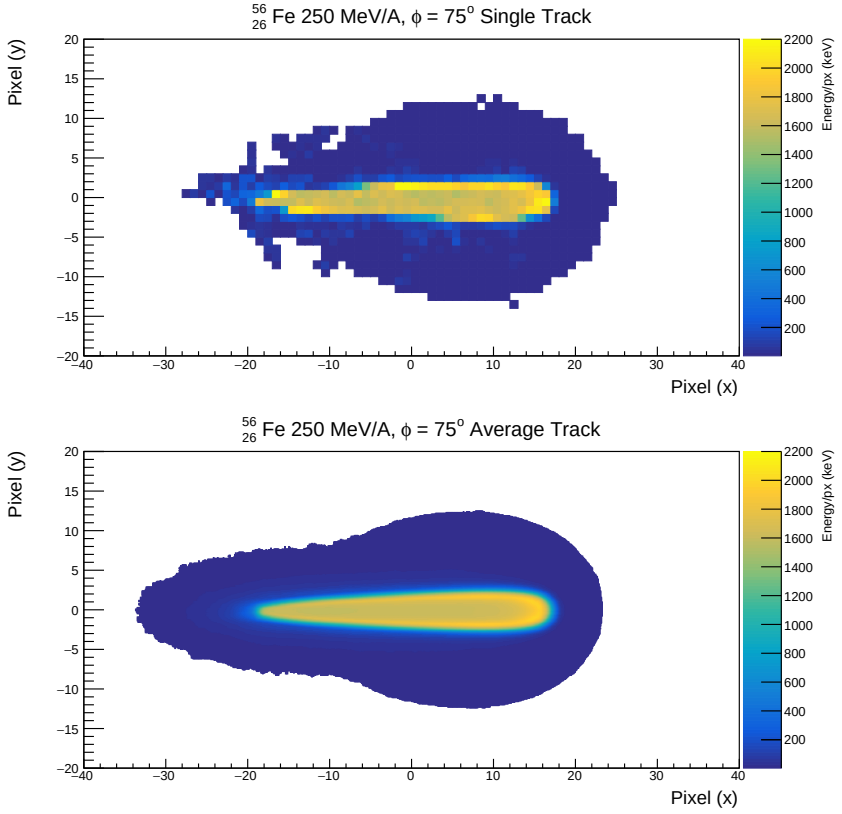

Figure 2. 180 MeV/A ^{56}Fe ion at 75°, single track (top) and averaged track over 10000 tracks (bottom). The volcano effect shows as a clear depression in the cluster core (approximate measured energy = 1600 keV per pixel) surrounded by a rim with a higher energy deposit. Each pixel has a pitch of 55 µm.

also calibrate the volcano effect using a large database of heavy ion data taken at the NASA Space Radiation Laboratory (NSRL) at Brookhaven National Laboratory (BNL), U.S.A. and at the Heavy Ion Medical Accelerator in Chiba (HIMAC) at the National Institute of Radiological Sciences in Chiba, Japan. This dataset is used to develop a per cluster correction for LET measurements as a function of track polar angles and LET which allows the Timepix to successfully measure LET values up to 500 keV µm^{-1}. Finally we investigate the per pixel response to very high input energies, deriving a pixelwise calibration curve that allows a per pixel correction to be applied to each cluster. We discuss the advantages and drawbacks to both of these techniques in correcting the volcano effect.

2 Pixel preamplifier response

A Timepix detector with a 500 µm thick silicon sensor was attached to a custom printed circuit board where one pixel has analogue outs for the preamplifier and signal comparator. This enables direct measurement of the response of the Timepix preamplifier to large input signals.

For input energies less than 800 keV the Timepix preamplifier behaves as designed with an approximately triangular response. Previous measurements [17] have shown that above approximately 800 keV the Timepix preamplifier exhibits an unexpected saturation effect whereby the triangular

2018 JINST 13 P11014

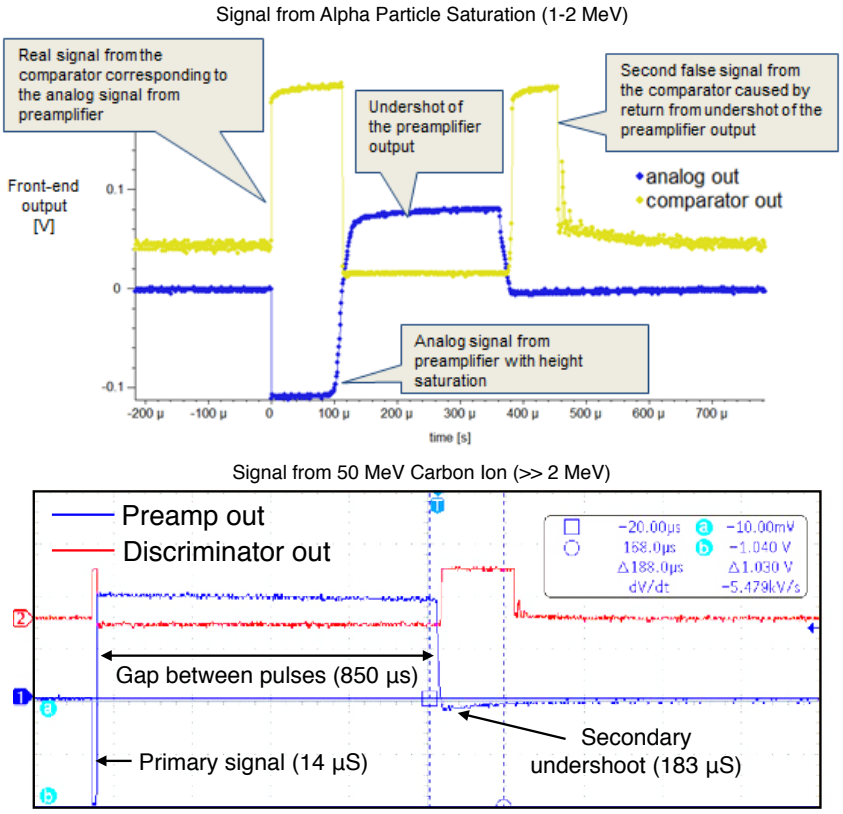

Figure 3. Oscillatory (top) and double (bottom) pulse structures observed from high input charges measured in a Timepix detector with 500 µm thick silicon sensor. The top figure shows the typical response of the Timepix preamplifier to energies from approximately 800 keV to approximately 2 MeV. (Reproduced from [17]. © 2014 IOP Publishing Ltd and Sissa Medialab srl.) The bottom figure shows the response to charges much higher than these vales. The principal differences between these figures are the shortening of the first pulse and the lengthening of the gap between the first and second pulses.

pulse is shortly followed by a second pulse. This additional pulse is associated with a slow exponentially shaped decay of the preamplifier which causes extra counts and hence erroneously high energy measurement. This effect can be reliably calibrated using monoenergetic protons following the procedure of Kroupa [18] allowing the Timepix preamplifier to measure input energies up to about 2000 keV. The response of the Timepix preamplifier to input charges beyond this value was previously not known.

Measurements of the preamplifier output were taken with 40 MeV Carbon ions in vacuum at the Tandem facility (a Van de Graaff facility) at BNL. These tracks stop in the first few microns of the sensor, depositing their full energy and producing large circular clusters. The preamplifier measurements show that in the case of a volcano the double pulse structure remains, but the first pulse shortens dramatically and is followed by a large gap before the second, oscillatory pulse. An example of the oscillatory pulse structure described by Kroupa et al. along with a volcano event is shown in figure 3. Compared to the original oscillatory pulse structure, in the case of a volcano, the first pulse is dramatically shortened and there is a much larger time gap before the second pulse.

2018 JINST 13 P11014

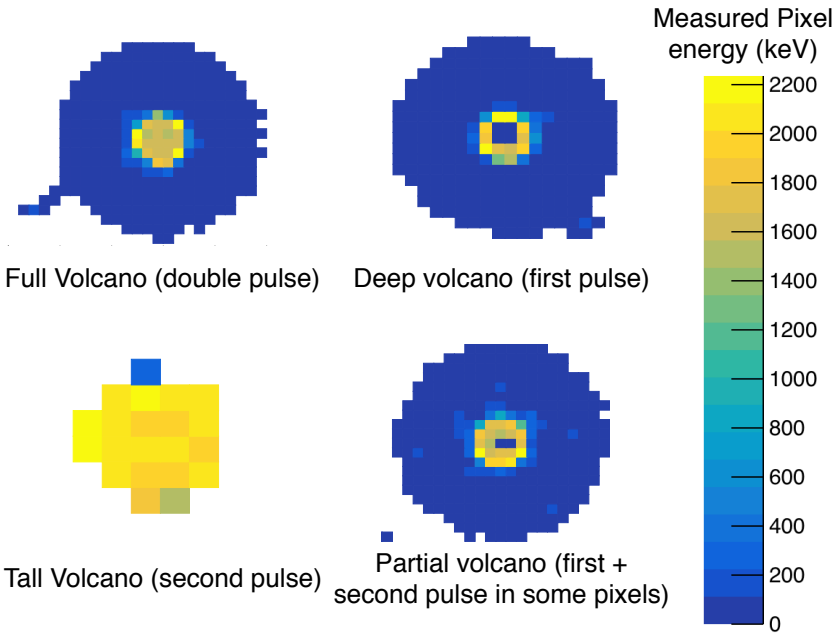

Figure 4. Taxonomy of different volcanos from 250 MeV ^{56}Fe ions at 0° polar angle measured with a 500 µm sensor. Full volcanos occur when both pulses are measured, deep volcanos are only from the first, tall volcanos from the second and partial volcanos are a combination of full and deep volcanos.

As the Timepix operates with a frame based readout (whereby the detector electronics only counts for a specific time window which is normally tuned by the user to keep the frame occupancy at a level where particle tracks do not overlap), the double pulse structure can lead to peculiar effects where one, both or some combination of pulses overlaps the start or end of a frame. This leads to a distinct taxonomy of different volcanos, most commonly measured in accelerator data. This is because the frame lengths used for typical accelerator measurements are often of the order of 1 mS to 10 mS, and hence of a similar size to the separation of the pulses.

We observe four different kinds of volcanos which are shown in figure 4. Full Volcanos which we define as the full response of the Timepix detector; Deep Volcanos which have a much deeper volcano effect with only a few counts in the central pixels; Tall Volcanos which are missing the low energy deposit regions of the cluster and Partial Volcanos which appear to be a mix between Full and Deep Volcanos. Armed with an understanding of the double pulse structure the interpretation is clear. Full Volcanos contain both pulses, Deep Volcanos only the first and Tall Volcanos the second. In the case of a Partial Volcano the frame has ended before the second pulse for some pixels.

An example LET spectrum from a measurement at HIMAC contains the Full Volcano peak, and two satellite peaks corresponding to the deep and tall volcanos, as well as a continuum of measurements from the partial volcanos. It is interesting to note that the Full Volcano peak has a reasonably narrow LET resolution (About 10% of measured LET), which suggests that the behavior of the volcano effect is largely deterministic and hence can be calibrated. This is in general seen throughout all of our measured accelerator data.

For our application measuring in space, count rates are generally low outside of rare periods of space weather and exposure to trapped radiation fields which consist mainly of protons. On

2018 JINST 13 P11014

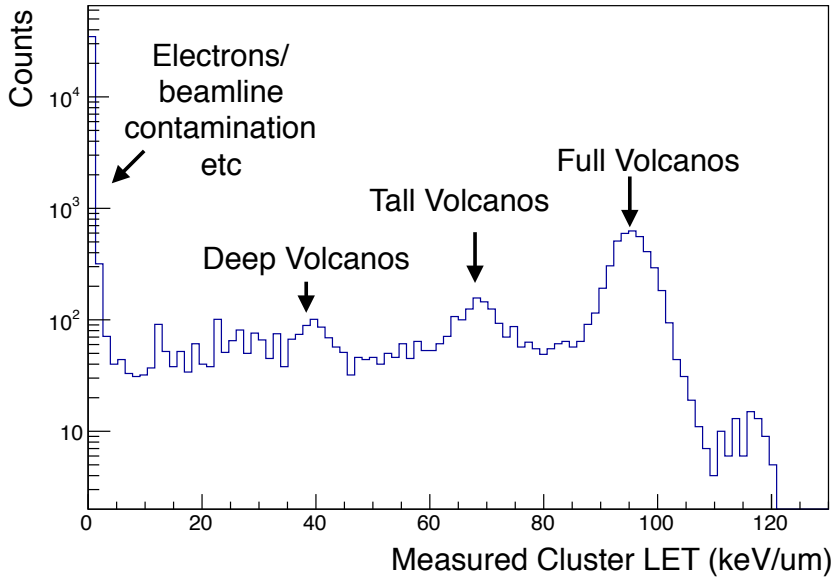

Figure 5. Typical measured accelerator LET spectrum from 250 MeV ^{56}Fe ions at 0° polar angle showing that different kinds of volcanos exhibit different characteristic LET measurements. Note that the theoretically expected LET value for this ion and energy is 500 keV µm^{-1}.

ISS exposure to trapped fields is limited to approximately 15 minutes a day, and on exploration class missions these will be limited to transits of the Van Allen belts. In typical space operation frame lengths are normally 1-4 seconds which is substantially longer than the frame lengths used to acquire data at accelerators. This means that the vast majority of volcanos observed in space are 'Full Volcanos' and that other types are very rare. This was verified by changing the acquisition time of our measurements, causing more deep and and tall volcanos to appear with short frame times and more full volcanos with long frames. Further discussion in this article will focus on Full Volcanos and measured LET values refer only to those in the Full Volcano peak. For our dataset this was achieved by cutting data outside of the full LET peak.

3 LET correction of Timepix data

A 500 µm thick Timepix detector was irradiated with a variety of ion species and energies at HIMAC and NSRL. The detector was setup in a similar way to the units on orbit; it was operated with a per pixel threshold of 4 keV and the Krummenacher current DAC which controls the discharge slope of the preamplifier was set to 2, this gives a pulse length in normal operation of approximately 0.3 µs/ke. The detector was calibrated using bench-top x-ray sources following the procedure of Jakubek [19] and 5 MeV monoenergetic protons following Kroupa et al. [18]. Theoretical most probable LET values were derived using a Geant4 [20, 21] simulation of the energy deposition and track lengths in a slab of silicon with a geometry corresponding to the Timepix sensor. The Geant4 simulation used the Quark Gluon String Plasma with Binary Ion Cascade for Hadronic Physics and the Livermore models for electromagnetic physics. The physics range cut after which secondary

2018 JINST 13 P11014

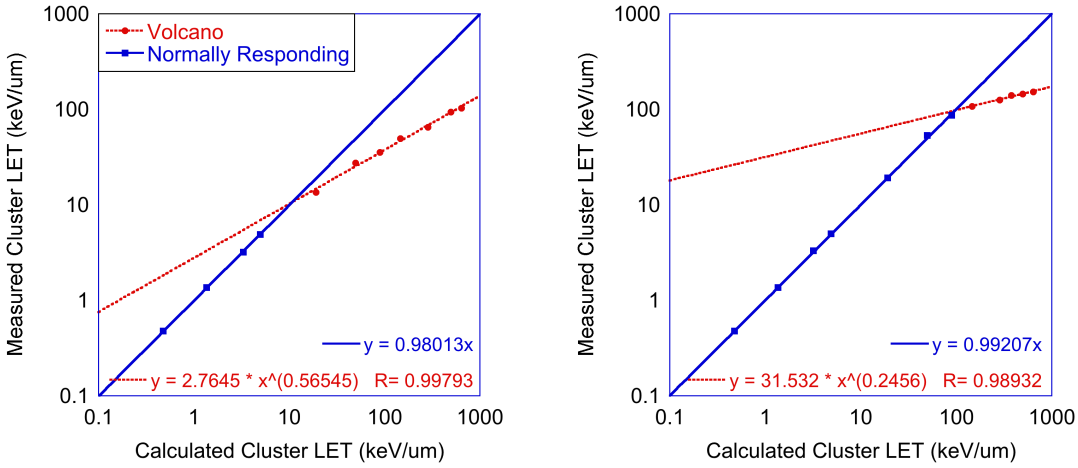

Figure 6. Measured vs calculated LET for tracks at 0° (left) and 75° (right) polar angle. In both cases the data calculated LET agrees with the measured LET up to a threshold value, when the data starts to follow a power law relationship.

particles are no longer tracked and their energy deposited locally was set at 2 µm in order to be significantly smaller than any of the geometry features in the simulation.

The relationship between the measured and predicted most probable LET for several different ion species/energy configurations (^{12}C, ^{16}O, ^{20}Ne, ^{40}Ar, ^{56}Fe) at 0 and 75 degree polar angle is shown in figure 6. This plot shows that in general the calculated LET can be related to the measured LET with a simple power law fit (i.e. $y = ax^b$) and has minimal if any dependence on the chosen ion species.

This power law relationship is seen for all angles tested. Figure 7 shows how the a and b parameters of the power law fit vary with polar angle. It is also interesting to calculate the LET value for which the volcano effect begins. This is done by calculating the intersection point of the power law fits with the normal response line and is also shown in figure 7. This plot shows that for the characterized assembly the volcano effect starts at approximately 10 keV µm^{-1} for low polar angle tracks, but for high polar angle tracks the normal response of the Timepix detector extends out to 100 keV µm^{-1}. This can be understood by consideration of the geometry of the system — Timepix pixels are 500 µm thick of approximately 9 times deeper than the pixel pitch of 55 µm. A track at 0 degrees polar angle traveling down the long axis of the pixel can deposit about 9 times more energy than one traveling along the short axis.

By interpolating the data used in figure 7 a LET based correction for any polar angle can be derived. This correction returns LET values within about 30% of the true LET value for all tested data and. A drawback of this method is the large amount of beamline data required for the calibration of one chip, which makes the relationships shown of academic interest, but quite impractical for general use. In the next section, we outline a more generally applicable method requiring far less calibration data.

2018 JINST 13 P11014

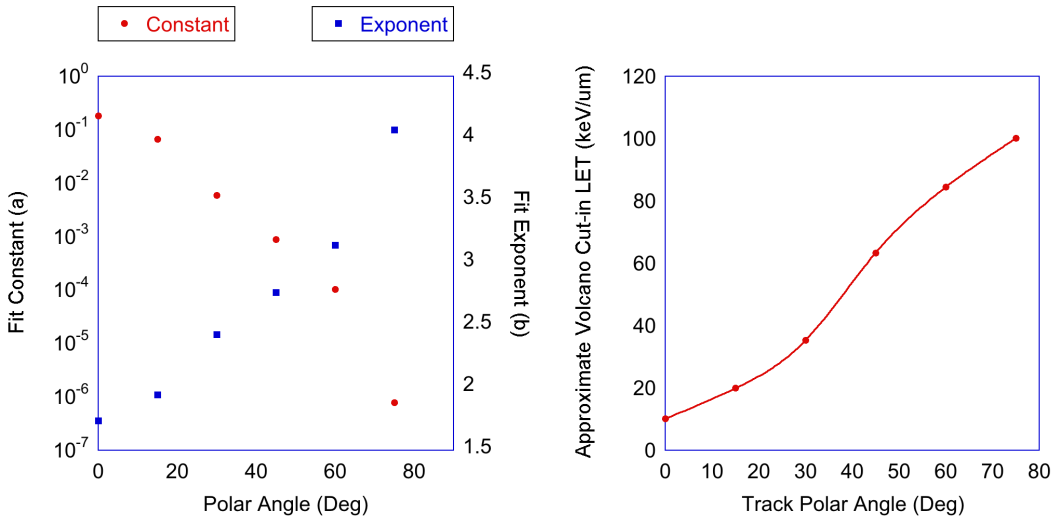

Figure 7. Constant and exponent of power law fits $y = ax^b$ of the measured vs theoretical LET dataset (left). Calculated volcano effect cutoff for tested assembly as a function of polar angle ϕ (right).

4 Per pixel calibration with monoenergetic protons

In this section we discuss an alternative methodology, whereby we derive a calibration curve from monoenergetic 8 MeV protons, which is used to correct clusters with a volcano effect on a per pixel basis. This correction uses 8 MeV protons generated at a Van de Graaff facility, which is already used for the 'advanced' calibration up to 2.2 MeV following Kroupa et al. [18]. This method therefore has a very significant logistical advantage over the whole cluster LET correction, requiring only one additional measurement as part of an existing calibration campaign.

A Timepix detector was exposed to monoenergetic 8 MeV protons in vacuum at the Tandem facility at BNL. 8 MeV protons have a range of 480 µm um in silicon and all stop near the bottom of the sensor. The potential therefore is for some of the protons to stop in the center of a pixel, depositing nearly all of their energy into one pixel.

The measured cluster volume spectrum is shown in figure 8. It is split by the number of pixels that may potentially be saturating, called 'hot' pixels in the figure. Hot pixels are defined as the number of pixels with an energy deposition over 1600 keV. The measured cluster volume increases with the number of hot pixels. Our interpretation of this is that when a proton stops in the center of a pixel it creates a large volcano in that pixel resulting in a single hot pixel and a large deposited energy deficit. However if a proton stops at the corner of 4 pixels it splits the charge evenly between the pixels, creating 4 hot pixels all of which are below the volcano threshold resulting in measurement of the full energy deposit of 8 MeV. 2 and 3 pixel clusters may have one or multiple volcanoing pixels.

The single hot pixel clusters can then be used to derive a calibration curve. This can be done by assuming that only a single pixel saturates and so the other pixels in the cluster are measuring energy correctly. We also know that the whole energy of the cluster which should always be 8 MeV as these protons should all stop. We can then calculate the energy that would be measured by the hot pixel if it were responding normally by subtracting the summed energy of the normal pixels from

2018 JINST 13 P11014

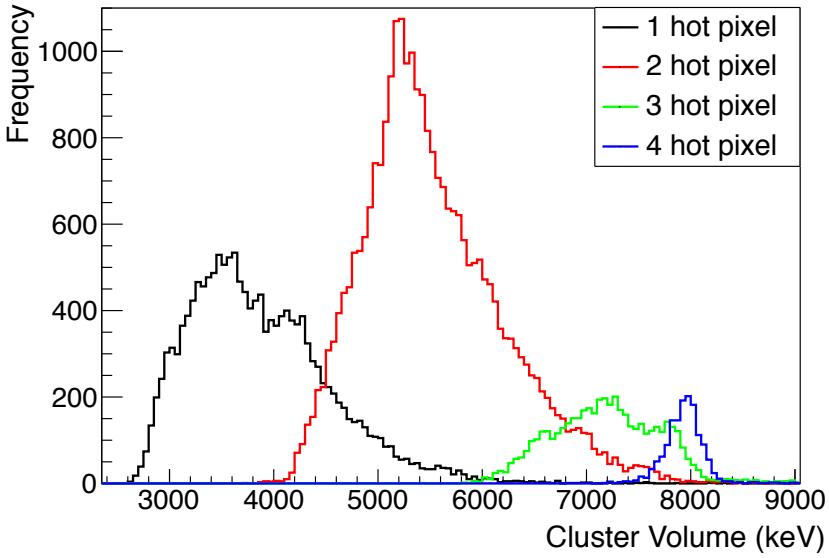

Figure 8. Cluster volume for 8 MeV protons at 0° degree polar angle as a function of the number of pixels > 1600 keV. All of these protons should stop in the sensor depositing the full 8 MeV of energy. The interpretation of this figure is that in the case of a single hot pixel the proton has stopped in the middle of a pixel depositing a large amount of energy which saturates the pixel. In the case of the 4 hot pixel cluster the proton has hit in the corner of all 4 pixels, sharing its energy between all them explaining the correct measurement of the full energy.

8 MeV. A calibration curve can then be derived by plotting this quantity against the actual measured energy, which is shown in figure 9. Also shown in figure 9 is a high energy extension shown in blue. This extension was calculated using a similar method, but with the tracks of 600 MeV/A ^{40}Ar ions. When near the back plane of the sensor these tracks are sufficiently narrow to be only one hot pixel wide, and the full volume of 8 MeV has been substituted for the average stopping power of Argon at this energy. As the actual deposited energy can fluctuate around this stopping power following the Landau-Vavilov distribution there is a larger spread of errors in this result. In general even for the highest LET clusters at low polar angles, we did not observe volcano depths in excess of 1600 keV to 1650 keV so it is likely that the volcano effect saturates around this value.

A schematic of the complete response of the Timepix pixel up to about 8 MeV can then be generated, which is shown in figure 10.

As the complete calibration curve for the Timepix is double valued one must have some method of selecting pixels that are saturating to correct the data on a per pixel basis. Unfortunately there is no a priori way to select a volcano pixel in the Timepix, which makes the correction of clusters with a volcano effect that is limited to one or two pixels quite difficult. For clusters with a well defined and distinguishable volcano there are a variety of feature recognition algorithms that could be used to attack the problem. We use a very simple scheme here, however it is clear that there are many other more sophisticated ways to go about solving this problem.

The essence of our scheme is that in principal Timepix clusters should have smooth continuous shapes, at least in the high energy deposit regions of the track. Our scheme is to apply the correction to all pixels in the cluster with energies greater than a threshold value of 1600 keV and then reverse

2018 JINST 13 P11014

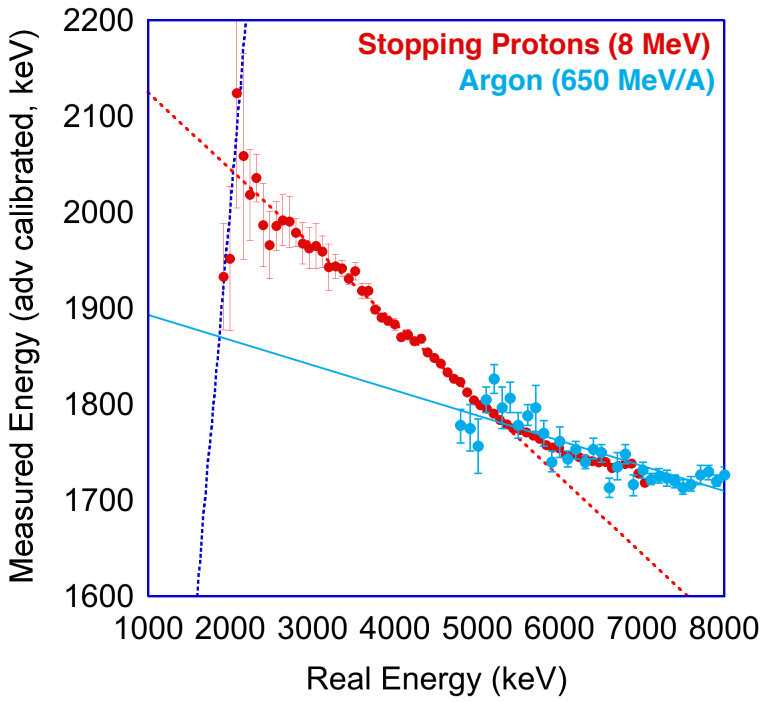

Figure 9. High energy calibration of the Timepix pixel. The curve from 2-5 MeV is derived by comparing the expected and measured values for 8 MeV protons with a single saturating pixel. The high energy extension is achieved using a similar method with 650 MeV ^{40}Ar ions at high polar angle. Here the full cluster energy is substituted for the expected energy deposit in some segment of the track. The expected (measured = real) response line is also shown (dashed, dark blue).

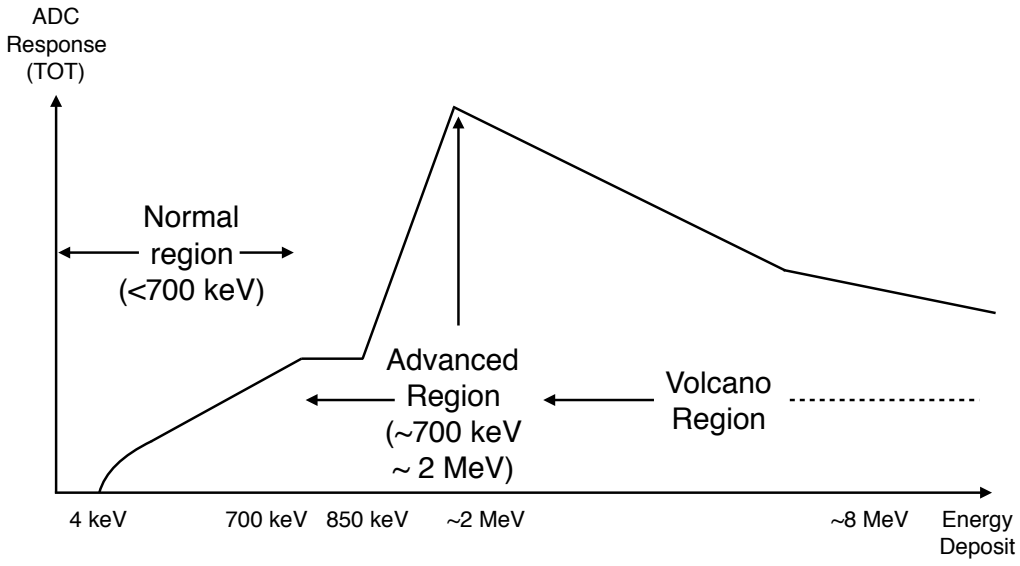

Figure 10. Schematic of the complete response of the Timepix front end to positive input charges. For a 500 µm thick silicon sensor the normal region can be calibrated with photons, the advanced region with 5 MeV protons and the volcano region with 8 MeV protons.

2018 JINST 13 P11014

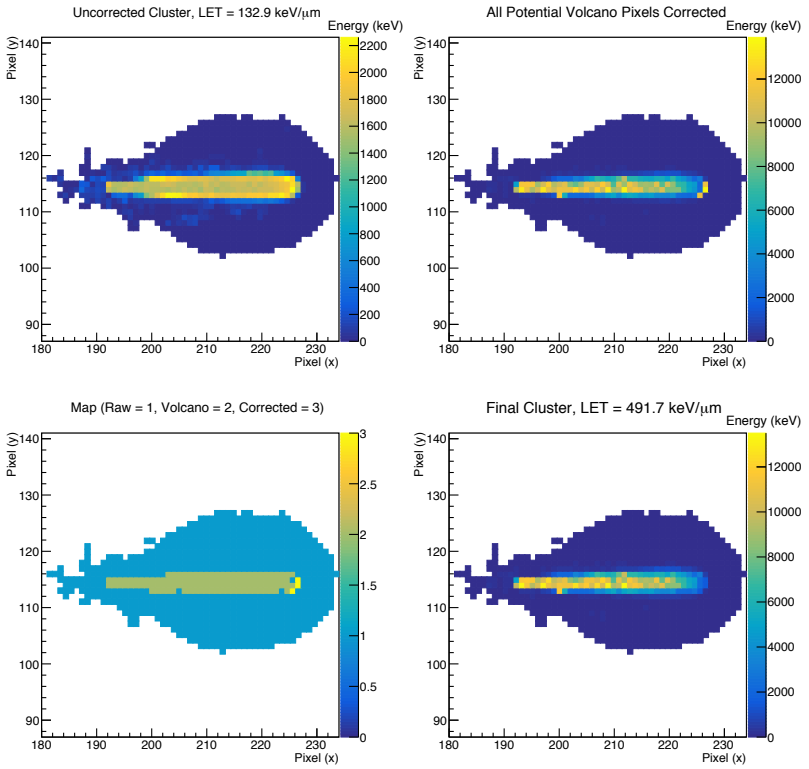

Figure 11. Cluster correction procedure for per pixel data on 250 MeV/A on ^{56}Fe ion, volcano response curve is applied to the raw cluster (top left) yielding a cluster with some miscorrected pixels (top right). The cluster is then searched for pixels with substantially higher corrected energy deposition than their neighbors (bottom left) which are corrected back to the raw value. This yields the final corrected cluster (bottom right).

this correction for pixels that are 'spikey' and have substantially higher calculated energies than their neighbors. Checking for 'spikey' pixels is done by checking if a pixel has greater than a tunable multiple n of the average corrected energy deposit of its neighboring pixels. A value of $n = 3$ worked best for our data as shown in the following text, but performance improvements may be possible by making n a function of the track polar angle or other parameters. An example corrected 250 MeV/A ^{56}Fe cluster is shown in figure 11.

The resultant LET spectra corrected with both the per pixel method and the whole LET power law method derived earlier in this paper is shown in figure 12.

A plot showing the result of the per pixel volcano correction for 5 different particle species as a function of polar angle is shown in figure 13. In general the performance is worse for low polar angle tracks. The principal reasons for this are two fold. For lower LET clusters at low polar angles only one or two pixels may volcano, and selecting these pixels correctly is difficult. For higher LET tracks low polar angle clusters can have considerably higher per pixel energy deposits for a particle with a given LET than high polar angles due to the geometry of the sensor, and that the correction curve shown in figure 9 seems to saturate at energies somewhere between 15 and 20 MeV.

In general the per pixel correction is able to compensate all tracks over 60 degrees polar angle with LET values up to 500 keV μm^{-1} in silicon. Figure 14 compares this with the previous

2018 JINST 13 P11014

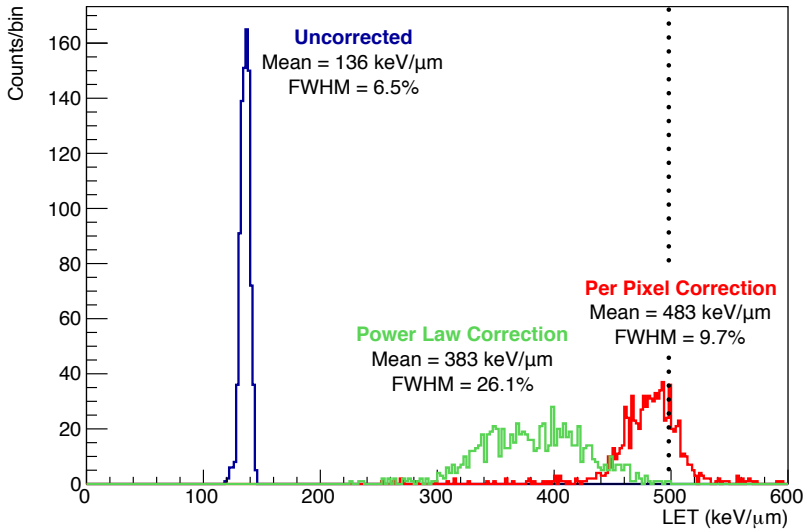

Figure 12. Raw and corrected LET spectra of 250 MeV/A ^{56}Fe at 75° polar angle. Corrections using the power law method (green) and per pixel method (red) are shown. The true LET is marked by the dotted line.

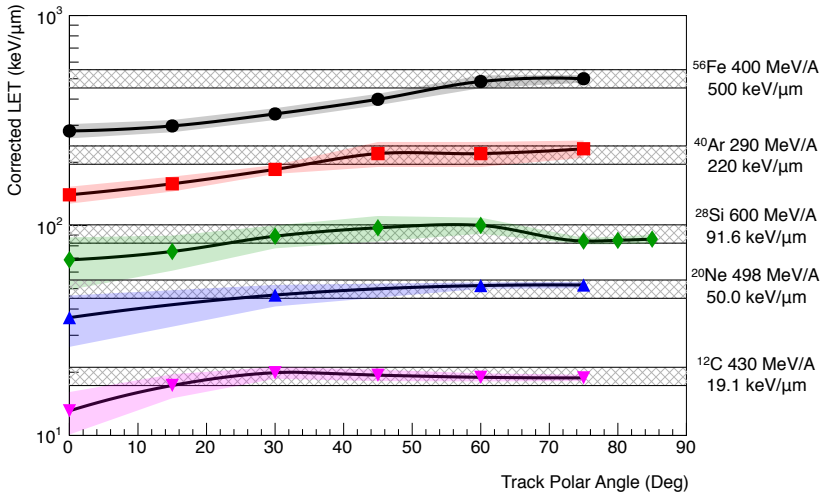

Figure 13. Result of per pixel LET correction for 5 different species as a function of track polar angle. The hatched bands show a region within 10% of the true LET value. Colored bands show the standard deviation of the corrected LET distribution. Lines are to guide the eye. In general the correction works best for higher polar angle tracks, with both narrower distributions and more accurate LET values.

performance of the chip by showing the fraction of LET measured as a function of LET and polar angle. The performance is clearly substantially improved for all LET values over 10 keV µm^{-1}.

5 Discussion and conclusions

The behavior of the Timepix when exposed to high input energy depositions and the so called volcano effect has been investigated in detail. The volcano effect presents as a double pulse

2018 JINST 13 P11014

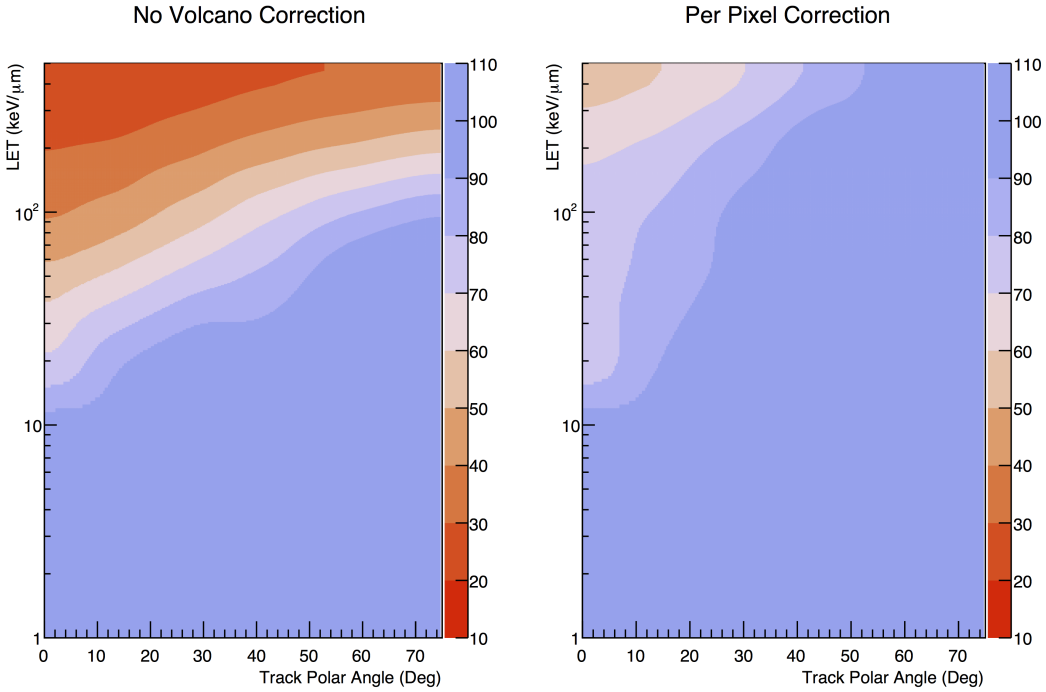

Figure 14. LET Measurement accuracy (%) as a function of true particle LET and polar angle with no (left) and per-pixel correction of the volcano effect (right). Color bands show in 10% increments from 100%, so the darkest blue color band covers all LET values within 10% of the true value. Figure achieved by interpolating between experimental datapoints for ^{1}H 100 MeV/A, ^{4}He 100 MeV/A, ^{12}C 430 MeV/A, ^{20}Ne 498 MeV/A, ^{40}Ar 290 MeV/A, ^{56}Fe 400 MeV/A and ^{56}Fe 250 MeV/A.

structure produced by the Timepix preamplifier. The long time period between these two pulses results in a several distinct kinds of observed volcanos when measured at accelerators, most of which are very rare when the detector is operated with long frame lengths. In general the volcano effect seems to be quite well behaved, and so can be corrected, at least in the tested Timepix assembly.

Two plausible schemes for correction of the volcano effect have been presented, one based on a whole LET solution and the other on a per pixel correction. Both corrections can substantially correct the volcano effect up to 500 keV μm^{-1} which covers the LET range of the cosmic ray spectrum up to Nickel.

Both methods have advantages and drawbacks. The power law LET method covers the whole LET and polar angle space, while the per pixel method exhibits some angle dependency, especially for polar angles less than 45°. The per pixel method generally exhibits superior accuracy and precision over its range of useful validity. The principal disadvantage of the whole LET method is that it requires a large amount of beamline data for a complete characterization. As such as this is quite prohibitive for general use. The datasets used in this article represent many shifts taken over two years at HIMAC and NSRL. In contrast the per pixel scheme requires a single measurement with 8 MeV protons to obtain a calibration curve for a chip which can be done using a Van de Graaff machine. As this same facility is already used for the energy calibration up to 2 MeV per pixel this is particularly advantageous.

2018 JINST 13 P11014

Given the ongoing interest and commitment to using Timepix devices for space dosimetry, understanding and correcting the volcano effect is a clear priority. Future work will focus on refinement of the techniques presented here, and understanding how the volcano effect varies between different Timepix assemblies.

Acknowledgments

The authors gratefully acknowledge the support of the staff at HIMAC in Chiba Japan as well as the National Space Radiation Laboratory and the Tandem Facility at Brookhaven National Laboratory, NY.

Portions of this study were presented at the 19th International Workshop on Radiation Imaging Detectors, held in Krakow Poland, 2–6 July 2017.

References

[1] X. Llopart, R. Ballabriga, M. Campbell, L. Tlustos and W. Wong, *Timepix, a 65k programmable pixel readout chip for arrival time, energy and/or photon counting measurements*, *Nucl. Instrum. Meth.* **A 581** (2007) 485.

[2] M. Campbell, *10 years of the Medipix2 Collaboration*, *Nucl. Instrum. Meth.* **A 633** (2011) S1.

[3] R. Ballabriga, M. Campbell and X. Llopart, *Asic developments for radiation imaging applications: The medipix and timepix family*, *Nucl. Instrum. Meth.* **A 878** (2018) 10.

[4] N. Stoffle, L. Pinsky, M. Kroupa, S. Hoang, J. Idarraga, C. Amberboy et al., *Timepix-based radiation environment monitor measurements aboard the International Space Station*, *Nucl. Instrum. Meth.* **A 782** (2015) 143.

[5] R. Gaza, M. Kroupa, R. Rios, N. Stoffle, E.R. Benton and E.J. Semones, *Comparison of novel active semiconductor pixel detector with passive radiation detectors during the NASA Orion Exploration Flight Test 1 (EFT-1)*, *Radiat. Me.* **106** (2017) 290.

[6] M. Kroupa, A. Bahadori, T. Campbell-Ricketts, A. Empl, S.M. Hoang, J. Idarraga-Munoz et al., *A semiconductor radiation imaging pixel detector for space radiation dosimetry*, *Life Sci. Space Res.* **6** (2015) 69.

[7] B. Lewis, R. Hanel, S. Bhattacharya, A. J. Ricco, E. Agasid, D. Reiss-Bubenheim et al., *BioSentinel: Monitoring DNA Damage Repair Beyond Low Earth Orbit on a 6U Nanosatellite*, in *Proceedings of Small Satellite Conference 2014*, Logan, Utah, U.S.A., 4–7 August 2014, SSC14-VII-3.

[8] S. Hoang, R. Vilalta, L. Pinsky, M. Kroupa, N. Stoffle and J. Idarraga, *Data Analysis of Tracks of Heavy Ion Particles in Timepix Detector*, *J. Phys. Conf. Ser.* **523** (2014) 12.

[9] S.P. George, C.T. Severino, E. Fröjdh, F. Murtas and M. Silari, *Measurement of an accelerator based mixed field with a Timepix detector*, 2015 *JINST* **10** P03005.

[10] S. George, *Dosimetric applications of hybrid pixel detectors*, Ph.D. thesis, University of Wollongong (2015).

[11] J.S. George, K.A. Lave, M.E. Wiedenbeck, W.R. Binns, A.C. Cummings, A.J. Davis et al., *Elemental Composition and Energy Spectra of Galactic Cosmic Rays During Solar Cycle 23*, *Astrophys. J.* **698** (2009) 1666.

2018 JINST 13 P11014

[12] M. Durante and F.A. Cucinotta, *Heavy ion carcinogenesis and human space exploration*, *Nat. Rev. Cancer* **8** (2008) 465.

[13] J.A. Zoutendyk, L.S. Smith and L.D. Edmonds, *Response of a DRAM to single-ion tracks of different heavy-ion species and stopping powers*, *IEEE Trans. Nucl. Sci.* **37** (1990) 1844.

[14] L.D. Edmonds, *Theoretical prediction of the impact of auger recombination on charge collection from an ion track*, *IEEE Trans. Nucl. Sci.* **38** (1991) 999.

[15] T. Campbell-Ricketts, M. Kroupa and L. Pinsky, *Spectroscopy of high-energy ions with Timepix3*, 2016 *JINST* **11** P11007.

[16] S.A. Al Azm, G. Chelkov, D. Kozhevnikov, A. Guskov, A. Lapkin, A.L. Fabelo et al., *Response of timepix detector with GaAs: Cr and Si sensor to heavy ions*, *Phys. Part. Nuclei Lett.* **13** (2016) 363.

[17] M. Kroupa, S. Hoang, N. Stoffle, P. Soukup, J. Jakubek and L.S. Pinsky, *Energy resolution and power consumption of Timepix detector for different detector settings and saturation of front-end electronics*, 2014 *JINST* **9** C05008.

[18] M. Kroupa, T. Campbell-Ricketts, A. Bahadori and A. Empl, *Techniques for precise energy calibration of particle pixel detectors*, *Rev. Sci. Instrum.* **88** (2017) 033301.

[19] J. Jakubek, *Precise energy calibration of pixel detector working in time-over-threshold mode*, *Nucl. Instrum. Meth.* **A 633** (2011) S262.

[20] GEANT4 collaboration, S. Agostinelli et al., *GEANT4: A Simulation toolkit*, *Nucl. Instrum. Meth.* **A 506** (2003) 250.

[21] J. Allison, K. Amako, J. Apostolakis, P. Arce, M. Asai, T. Aso et al., *Recent developments in Geant4*, *Nucl. Instrum. Meth.* **A 835** (2016) 186.

2018 JINST 13 P11014